Development of a new Near-wall Reynolds Stress Turbulence Model for Jet Impingement Heat Transfer Prediction

Miloš Banjac
Teaching and Research Assistant

Bogosav Vasiljević
Associate Professor

University of Belgrade
Faculty of Mechanical Engineering

The newly proposed Reynolds-stress turbulence model (second moment closure) was created by transforming the "standard" high-Reynolds Isotropisation-of-Production turbulence model into its low-Reynolds version and by introducing a new additional wall-reflection term ${}^{*}\mathcal{R}_{\tau,ij}^{II,\mathrm{w}}$. *Transformation from high- to low-Reynolds turbulence model was carried out by including the previously neglected influence of molecular diffusion i.e. by introducing the appropriate terms and functions into Reynolds stress and turbulent dissipation rate transport equation. The new additional "rapid" wall-reflection term* ${}^{*}\mathcal{R}_{\tau,ij}^{II,\mathrm{w}}$, *that was modeled in accordance to the real physical situation, encompassed the "atypical" so-called pressure-echo effect, i.e. the "atypical" redistribution of turbulent stress in the vicinity of the stagnation point of an impinging jet.*
In contrast to "standard" linear near-wall two-equation turbulence models, the newly proposed Reynolds-stress turbulence model gives essentially better predictions of turbulent kinetic energy field and considerably better predictions of local Nusselt number. Compared with the "standard" high-Reynolds turbulence stress models, the proposed turbulence model demonstrates considerably better prediction of turbulent stress field in the vicinity of impinging jet stagnation point, slightly better prediction of mean velocity field, and also enables prediction of local Nusselt number.

Keywords: *Impinging jet, Low-Reynolds-stress turbulence model, redistribution of turbulent stress, local Nusselt number.*

1. INTRODUCTION

The high heat transfer rates that can occur in the stagnation region of impinging jets have induced their use in a wide variety of applications. These include cooling gas turbine components and the outer wall of combustors, cooling electronic equipment, annealing metal and plastic sheets, tempering glass and freezing tissue in cryosurgery.

The impinging jet flow, despite its relatively simple geometry, exhibits extremely complex flow characteristics. Among others, the flow around the stagnation point is nearly irrotational and there is a large total strain along the streamline (Fig. 1). Away from the core of the jet there is a substantial curvature of the streamline. Also, the laminar boundary layer that exists in the vicinity of the stagnation point is transforming to turbulent and outside the stagnation region, along the plate, flow forms a wall jet boundary layer. Simultaneous effect of a large number of parameters, makes very difficult accurate prediction of flow and corresponding heat transfer in classical, dimensionless number correlations, based way. The overall heat transfer performance of jet impingement configuration has been examined in numerous experiments, many of which have been cited by Viskanta (1993) and Holger (1977).

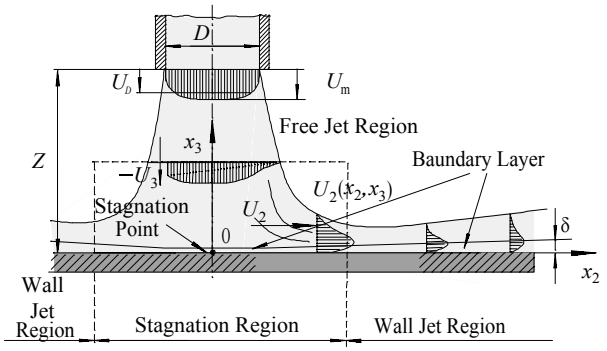

Figure 1. Flow field of impinging flow (schematic)

The impinging turbulent jet is also an interesting flow from another, rather different standpoint. Namely, almost the all turbulent models were developed for shear turbulent flows, with reference to flows parallel to wall. By using some of these turbulence models it is possible to get very correct prediction of flow characteristics for different configurations and a very wide range of turbulent flows. These models, which show high level of "universality" and which are colloquially called "standard" or "common", are very often built in every commercial CFD software. But, it also turned out that numerical calculation carried out by

Received: Septembar 2004, Accepted: November 2004.

Correspondence to: Miloš Banjac
Faculty of Mechanical Engineering,
Kraljice Marije 16, 11120 Belgrade 35, Serbia and Montenegro
E-mail: mbanjac@mas.bg.ac.yu

using these "standard" turbulence models for impinging jet flow simulation showed significant disagreement with relevant experimental data particularly for the local heat transfer coefficient. This disagreement is especially large in the stagnation region. In Fig. 2 we are compared the experimental results of Baughun (1992) for heat transfer along the plate and results of own numerical simulation for four different "standard" low Reynolds two-equations turbulence models.

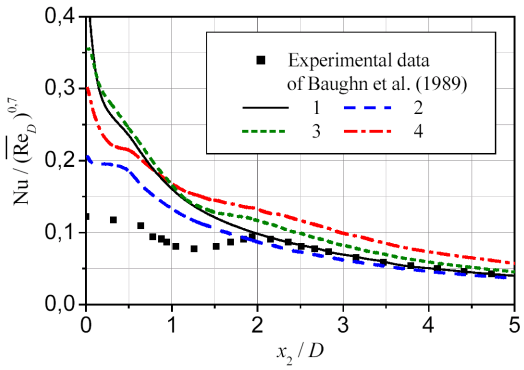

Figure 2. Variation of scaled Nusselt number with radius for Low Reynolds Number Models ($Z/D=2$, $\overline{\mathrm{Re}}_D = 23000$):

1. ***Basic*** $k-\varepsilon$ ***Launder-Spalding model;***
2. ***Basic*** $k-\omega$ ***Wilcox model;***
3. ***Lam-Bremhorst*** $k-\varepsilon$ ***model;***
4. ***Chen-Kim Modified*** $k-\varepsilon$ ***model.***

In this work, with intention to overcome shortcomings of those "standard" turbulence models, a new Reynolds-stress turbulence model is proposed. After carrying out a detailed analysis and because of the basic weakness of the Boussinesq's eddy-viscosity stress-strain relation, an idea that any corrections of any two-equation turbulence models can lead to better prediction was abandoned. The new model was created by transforming the "standard" Launder, Reece and Rodi (1975) high-Reynolds Isotropisation-of-Production turbulence Model (IP). IP model was chosen for transformation, as a model which still exist in commercial CFD software PHOENICS and as a model which can represent the most superior group of models - Reynolds-stress turbulence models (RSTM).

The first set of transformations of IP model was refered to transformations from high-Reynolds IP model into its low-Reynolds version (IP1 model). The second transformation was refered to introducing a new additional wall-reflection term ${}^{*}\mathcal{R}_{\tau,ij}^{w,II}$ (IP2 model).

2. AVAILABLE EXPERIMENTAL DATA

The performance of all models has been assessed by comparing the numerically predicted results to corresponding experimental data of Baughun at al. (1989) and Cooper at al. (1993). This comparison was related onto four cases, for two and six jet diameters to plate spacing and for two different Reynolds numbers, $\overline{\mathrm{Re}}_D = 23000$ and $\overline{\mathrm{Re}}_D = 70000$.

The most important features of experiments of these authors was achieving the fully developed pipe flow at the exit and that the nozzle lip was thick and square cut[1)].

3. GOVERNING EQUATIONS

3.1. The basic balance equations

In accordance to real physical situation and under adequate assumptions (air is Newtonian fluid and turbulent flow is incompressible, stationary and with neglected buoyancy), the governing equations of fluid motion can be written in Cartesian tensor notation as:

- continuity equation

$$\partial U_i / \partial x_i = 0\,, \tag{1}$$

- Reynolds averaged Navier-Stokes equations

$$\frac{\partial}{\partial x_j}(\rho U_i U_j) = -\frac{\partial P}{\partial x_i} + \frac{\partial}{\partial x_j}[\mu_f(\frac{\partial U_i}{\partial x_j} + \frac{\partial U_j}{\partial x_i}) - \rho\overline{u_i u_j}]\,, \tag{2}$$

and the governing equation of mean enthalpy (energy equation) as:

$$\frac{\partial}{\partial x_j}(\rho U_j H) = U_i \frac{\partial P}{\partial x_i} + \mu_f \Psi_\mu(U_i) + \mu_f \Psi_\mu(u_i) + \\ + \frac{\partial}{\partial x_i}(a_f \frac{\partial H}{\partial x_i} - \rho\overline{h u_i})\,. \tag{3}$$

3.2. Basic High-Reynolds Isotropisation-of-Production turbulence Model – transport equations

In the case of all high-Reynolds second moment closure approach, the unknown Reynolds stresses ($\tau_{ij} = -\rho\overline{u_i u_j}$) are obtained from the following transport equation:

$$U_k \frac{\partial \tau_{ij}}{\partial x_k} = \mathcal{D}^u_{\tau,ij} + \mathcal{P}^U_{\tau,ij} - \mathcal{E}_{\tau,ij} + \mathcal{R}_{\tau,ij}\,. \tag{4}$$

where $\mathcal{D}^u_{\tau,ij}$ represents diffusive transport of τ_{ij} by velocity fluctuation and it is modelled by using the Daly-Harlow model (1970):

$$\mathcal{D}^u_{\tau,ij} = -\frac{\partial}{\partial x_k}(C_s \frac{k}{\rho\varepsilon}\tau_{kl}\frac{\partial \tau_{ij}}{\partial x_l})\,. \tag{5}$$

Wherein, C_s is an empirical constant, k is the turbulent kinetic energy and ε is the dissipation of k.

The stress production term $\mathcal{P}^U_{\tau,ij}$ needs no approximation and is defined by:

$$\mathcal{P}^U_{\tau,ij} = -(\tau_{im}\frac{\partial U_j}{\partial x_m} + \tau_{jm}\frac{\partial U_i}{\partial x_m})\,. \tag{6}$$

The viscous destruction correlation $\mathcal{E}_{\tau,ij}$ is modeled by

[1)] Latter experimental results by Baughun et. all (1992) and some other authors which were also made in an impinging air jet, but with different imaging system (for both, temperature and velocity measurement), confirmed their previous results. This confirmation enabled that their experimental data become part of ERCOFTAC-IAHR Data Base (*European Research Community on Flow, Turbulence and Combustion – International Association of Hydraulic Research*).

assuming local isotropy (Roota, 1951):

$$\mathcal{E}_{\tau,ij} = -\frac{2}{3}\rho\varepsilon\delta_{ij}, \tag{7}$$

and the pressure-strain correlation $\mathcal{R}_{\tau,ij}$ is modeled as a sum of four contributions[2] (Shir, 1973):

$$\mathcal{R}_{\tau,ij} = \mathcal{R}^{I}_{\tau,ij} + \mathcal{R}^{II}_{\tau,ij} + \mathcal{R}^{w,I}_{\tau,ij} + \mathcal{R}^{w,II}_{\tau,ij}. \tag{8}$$

The first contribution, marked as $\mathcal{R}^{I}_{\tau,ij}$, represents the so-called "slow" (or turbulent-turbulent) part of pressure-strain correlation and term $\mathcal{R}^{w,I}_{\tau,ij}$ is its wall-reflection correction. $\mathcal{R}^{II}_{\tau,ij}$ is the so-called "rapid" (or mean-strain) part of pressure-strain correlation and $\mathcal{R}^{w,II}_{\tau,ij}$ is its wall-reflection correction. In all models RSTM, the wall-correction terms to the pressure strain are the same and they have following form (Shir, 1973):

$$\mathcal{R}^{w,I}_{\tau,ij} = C_{w1}\frac{\varepsilon}{k}f_w(\tau_{km}n_k n_m\delta_{ij} - \frac{3}{2}\tau_{ki}n_k n_j - \frac{3}{2}\tau_{kj}n_k n_i) \tag{9}$$

and

$$\mathcal{R}^{w,II}_{\tau,ij} = C_{w2}f_w(\mathcal{R}^{II}_{\tau,km}n_k n_m\delta_{ij} - \frac{3}{2}\mathcal{R}^{II}_{\tau,ki}n_k n_j - \frac{3}{2}\mathcal{R}^{II}_{\tau,kj}n_k n_i) \tag{10}$$

where, C_{w1} and C_{w2} are empirical constants; n_k is the unit vector normal to wall, and f_w is the wall-damping function. The wall-damping function is computed from:

$$f_w = C_w\ell / y_n,$$

where: y_n is the normal distance from the wall; $C_w = y_{nw}/\ell$ at the near-wall grid point; and ℓ is the turbulence length scale given by:

$$\ell = C_D k^{3/2}/\varepsilon,$$

where, C_D is an empirical constant. The value chosen for C_w ensures that f_w is unity in near-wall turbulence.

Also, in all RSTM[2] the "slow" part of pressure-strain correlation $\mathcal{R}^{w,I}_{\tau,ij}$ is modeled as (Launder, 1975):

$$\mathcal{R}^{I}_{\tau,ij} = -C_1\frac{\varepsilon}{k}(\tau_{ij} + \frac{2}{3}\delta_{ij}\rho k), \tag{11}$$

wherein C_1 is an empirical constant. Regarding to model for "rapid" part of pressure-strain correlation $\mathcal{R}^{II}_{\tau,ij}$, there are three similar models: Quasi-Isotropic Model (QI model) by Launder, Reece and Rodi (1975), Isotropisation-of-Production Model (IPY model) of Younis (1984) and Isotropisation-of-Production Model (IP model) by Launder, Reece and Rodi (1975). In the case of IP turbulence model $\mathcal{R}^{II}_{\tau,ij}$ is modeled as:

$$\mathcal{R}^{II}_{\tau,ij} = -C_2(\mathcal{P}^{U}_{\tau,ij} - \frac{1}{3}\delta_{ij}\mathcal{P}^{U}_{\tau,kk}), \tag{12}$$

where, C_2 is empirical constant (Table 1).

In all high-Reynolds RSTM, the turbulence energy dissipation rate ε is computed from modeled transport equation:

$$\rho U_i\frac{\partial\varepsilon}{\partial x_i} = \mathcal{D}^{u}_{\varepsilon} + \mathcal{P}^{s}_{\varepsilon} - \mathcal{E}_{\varepsilon}, \tag{13}$$

where, $\mathcal{D}^{u}_{\varepsilon}$ represents diffusive transport, and is modeled by:

$$\mathcal{D}^{u}_{\varepsilon} = -\frac{\partial}{\partial x_i}(C_\varepsilon\rho\frac{k}{\varepsilon}\tau_{ij}\frac{\partial\varepsilon}{\partial x_j}). \tag{14}$$

Production of dissipation by vortex stretching $\mathcal{D}^{s}_{\varepsilon}$ and destruction of dissipation by viscous diffusion $\mathcal{E}_{\varepsilon}$ are modeled together (Hanjalić, 1976):

$$\mathcal{P}^{s}_{\varepsilon} - \mathcal{E}_{\varepsilon} = \rho\frac{\varepsilon}{k}\left(\frac{1}{2}C_{\varepsilon1}\mathcal{P}^{U}_{\tau,kk} - C_{\varepsilon2}\varepsilon\right). \tag{15}$$

In the foregoing, C_ε, $C_{\varepsilon1}$ and $C_{\varepsilon2}$ are empirical constants.

Table 1. Empirical constants of IP turbulence model

C_s	C_1	C_2	C_{w1}	C_{w2}
0,22	1,80	0,60	0,50	0,30

$C_D = (C_\mu C_D)^{0,75}$	C_ε	$C_{\varepsilon1}$	$C_{\varepsilon2}$
$C_\mu C_D = 0,065$	0,18	1,45	1,90

3.3. Generalized gradient-diffusion hypothesis model for turbulent energy flux $-\rho\overline{hu_i}$

The time-averaged dissipation function $\Psi_\mu(U_i)$ and the turbulent energy dissipation function $\Psi_\mu(u_i)$ from the equation of mean enthalpy (3) are modeled together (Spalding, 1999) i.e. replaced with:

$$\mu_f\Psi_\mu(U_i) + \mu_f\Psi_\mu(u_i) = 2\tau_{ij}S_{ij}, \tag{16}$$

where S_{ij} is the deformation tensor:

$$S_{ij} = (\partial U_i/\partial x_j + \partial U_j/\partial x_i)/2.$$

In accordance with the generalized gradient-diffusion hypothesis model, turbulent energy flux $-\rho\overline{hu_i}$ is replaced with:

$$-\rho\overline{hu_i} = C_\theta\rho\frac{k}{\varepsilon}\overline{u_iu_j}\frac{\partial H}{\partial x_j} = -C_\theta\frac{k}{\varepsilon}\tau_{ij}\frac{\partial H}{\partial x_j}. \tag{17}$$

3.4. Equation of state

Under the assumption that fluid has constant thermo-physical properties (molecular viscosity μ_f, thermal conductivity λ_f and c_p specific heat capacity at constant pressure), the three conservation equations (1-3), two transport equation (4, 13), two hypotheses (16, 17) and equation of state for ideal-gas:

$$\rho = P/RT, \quad H = c_pT, \tag{18), (19}$$

create a mathematically closed system.

[2] Except Speziale, Sarkar and Gatski (1991) turbulent model (SSG)

4. LOW-REYNOLDS VERSION OF THE ISOTROPISATION-OF PRODUCTION TURBULENCE MODEL (IP1)

In order to acquiring reliable numerical data inside the velocity as well as the temperature boundary layer, it was necessary to include in transport equations (4, 13) the previously neglected influence of molecular viscosity. After numerous attempts, by using the well-known models for corresponding terms, IP model widened and corrected in the way demonstrated below, has given acceptable results.

The Reynolds stress transport equation was corrected in two terms:

$$U_k \frac{\partial \tau_{ij}}{\partial x_k} = \mathcal{D}^u_{\tau,ij} + \underbrace{\mathcal{D}^{\nu}_{\tau,ij}}_{\text{New term}} + \mathcal{P}^U_{\tau,ij} - \underbrace{\mathcal{E}_{\tau,ij}}_{\text{Corrected term}} + \mathcal{R}_{\tau,ij} . \quad (20)$$

The term $\mathcal{D}^{\nu}_{\tau,ij}$, that describe molecular diffusion of Reynolds stress was added in its non-modeled form:

$$\mathcal{D}^{\nu}_{\tau,ij} = \frac{\partial}{\partial x_k}\left(\nu \frac{\partial \tau_{ij}}{\partial x_k}\right), \quad (21)$$

and dissipation rate tensor $\mathcal{E}_{\tau,ij}$ was corrected with damping function f_s (Hanjalić, 1976):

$$\mathcal{E}_{\tau,ij} = -\left[\frac{2}{3}\rho\varepsilon(1-f_s)\delta_{ij} - f_s\,\varepsilon\frac{\tau_{ij}}{k}\right], \quad (22)$$

where function factor f_s is:

$$f_s = (1+\mathrm{Re_t}/10)^{-1},$$

and Reynolds turbulent number $\mathrm{Re_t}$ is defined as:

$$\mathrm{Re_t} \equiv k^2/(\nu\varepsilon).$$

The transport equation for the turbulence energy dissipation rate ε was corrected in three terms:

$$\rho U_i \frac{\partial \varepsilon}{\partial x_i} = \mathcal{D}^u_{\varepsilon} + \underbrace{\mathcal{D}^{\nu}_{\varepsilon}}_{\text{Added term}} + \mathcal{P}^s_{\varepsilon} + \underbrace{\mathcal{P}^U_{\varepsilon}}_{\text{Added term}} - \mathcal{E}_{\varepsilon} + \underbrace{\mathcal{P}^{\Omega}_{\varepsilon}}_{\text{Added term}}$$

The term $\mathcal{D}^{\nu}_{\varepsilon}$, that represents molecular diffusion of ε was added in its non-modeled form:

$$\mathcal{D}^{\nu}_{\varepsilon} = \mu\frac{\partial^2\varepsilon}{\partial x_k^2} \quad (23)$$

and added term $\mathcal{P}^U_{\varepsilon}$, which represents the production of dissipation by mean strains was modeled together with the production of dissipation by vortex stretching term $\mathcal{P}^s_{\varepsilon}$ and term $\mathcal{E}_{\varepsilon}$ that represents the destruction of dissipation by viscous diffusion (Hanjalić, 1976):

$$\mathcal{P}^U_{\varepsilon} + (\mathcal{P}^s_{\varepsilon} - \mathcal{E}_{\varepsilon}) = \rho\frac{\varepsilon}{k}\left(\frac{1}{2}C_{\varepsilon 1}\mathcal{P}^U_{\tau,qq} - C_{2\varepsilon}f_{\varepsilon}\hat{\varepsilon}\right). \quad (24)$$

In the foregoing equation f_{ε} is the Patel's damping function (Patel, 1985):

$$f_{\varepsilon} = 1 - \frac{2}{9}\exp\left[\left(-\mathrm{Re_t}/2\right)^2\right], \quad (25)$$

and $\hat{\varepsilon}$ the isotropic part of dissipation rate of turbulent kinetic energy:

$$\hat{\varepsilon} = \varepsilon - 2\nu_f\left(\partial k^{0,5}/\partial x_k\right). \quad (26)$$

The "standard" model for non-homogeneous production of ε, term $\mathcal{P}^{\Omega}_{\varepsilon}$ (Hanjalić, 1976):

$$\mathcal{P}^{\Omega}_{\varepsilon} = \mu_f C_{\varepsilon 4}\frac{k}{\varepsilon}\overline{u_j u_k}\frac{\partial^2 U_i}{\partial x_j \partial x_l}\frac{\partial^2 U_i}{\partial x_k \partial x_l}, \quad (27)$$

in keeping with suggestion of Craft's (Craft, 1991), was replaced with Yap's corrections:

$$\mathcal{P}^{\Omega}_{\varepsilon} \rightarrow S_{Yap} = \max\left[0;\ 0{,}83\rho\left(\frac{\ell}{\ell_e}-1\right)\left(\frac{\ell}{\ell_e}\right)^2\frac{\varepsilon^2}{k}\right], \quad (28)$$

where $\ell_e = \mathrm{C}_D y_n/\kappa$.

In this way, high-Reynolds IP model was successfully transformed into its Low-Reynolds version.

5. BOUNDARY CONDITIONS

The boundary conditions and the solution domain are summarized in Fig. 3 and Fig. 4.. At the jet discharge, the flow is fully developed and isothermal. The inlet condition is obtained by the preceding, separate computation of fully developed pipe flow. For boundary conditions near the wall the corresponding "wall-functions" were used. In the case of simulation with IP model, the non-dimensional distance of the near-wall node from the wall was $6 < y_w^+ < 11{,}63$ and in the case of IP1 model $y_w^+ < 1$.

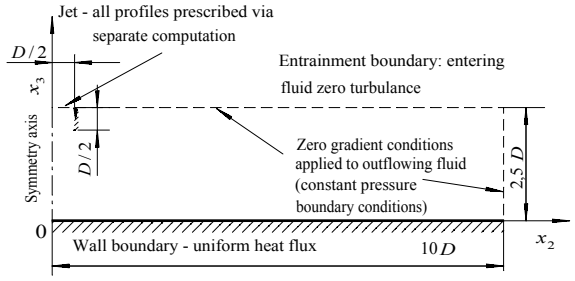

Figure 3. Summary of boundary conditions

6. NUMERICAL PROCEDURE

Computations were done with PHOENICS computer program. This solver is based on finite volume solution of elliptic mean momentum, energy and turbulent transport equations. It uses a staggered mesh and the Patankar's SIMPLE algorithm for successively correcting the pressure and field to secure compliance with continuity.

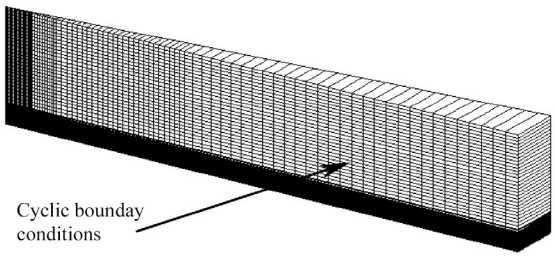

Figure 4. Solution domain and disposition of cells for the $Z/D = 2$, $\overline{\mathrm{Re}}_D = 23000$ case

7. NUMERICAL RESULTS

Comparison of certain characteristic experimental data for velocity profiles, turbulence intensity and Nusselt number and corresponding data obtained by numerical computation for the $\overline{\mathrm{Re}}_D = 23000$ and $Z/D = 2$ regime, are shown in Figures 5 to 8. The rest of results and the results for other flow regimes of streaming are presented in (Banjac, 2004).

It is easy to observe good agreement between experimental and numerical data for velocity profiles at all radial positions, as well as unsatisfactory agreement for turbulent velocity profiles and local Nusselt number in radial position near the stagnation point. IP and IP1 turbulence models gave especially wrong bad predictions for Reynolds stress normal to the wall, again in the vicinity of symmetry axis.

8. ANALYSIS

The pressure-strain correlation:

$$\mathcal{R}_{\tau,ij} = -\overline{p\left(\partial u_i/\partial x_j + \partial u_j/\partial x_i\right)}$$

that, as its name suggests, is the time-averaged product of the turbulent kinematics pressure and strain rate, plays a crucial role in the budget of Reynolds stress tensor τ_{ij}. Since in incompressible flow, its trace is zero, it describes redistribution of turbulent energy among the normal stresses and diminishing the correlation between off-diagonal components. There are two contributions to this process, one associated with a nonlinear interaction $\mathcal{R}^{I}_{\tau,ij}$ – the "slow" part of $\mathcal{R}_{\tau,ij}$ (11), and the second involving mean strains, $\mathcal{R}^{II}_{\tau,ij}$ the "rapid" part of $\mathcal{R}_{\tau,ij}$ (12).

In the "standard" second-moment closures for turbulent stress field, so in IP and IP1 model as well, a wall-reflection correction: $\mathcal{R}^{\mathrm{w}}_{\tau,ij} = \mathcal{R}^{\mathrm{w},I}_{\tau,ij} + \mathcal{R}^{\mathrm{w},II}_{\tau,ij}$, is added to the model of pressure-strain correlation $\mathcal{R}_{\tau,ij}$ in computing flow near the walls. Its role is to describe process of reducing the level of turbulent velocity fluctuations normal to the wall and, through the strong intercoupling among the Reynolds stress components, to reduce generally level of turbulent mixing.

In all cases of shear flows (directed parallel to the wall) previously mentioned RSTM showed excellent prediction. When however, the scheme of those models, so that IP and IP1 model as well, was applied to the axisymmetric impinging jet, it led to wrong, too excessive predictions of levels of the normal-to-wall turbulent stresses in the vicinity of the stagnation point (Fig. 7). This different behavior can be explained by examining the "contribution" that the term makes in two different cases – channel flow (a represent ant of shear flow – Fig. 9) and impinging flow (Fig. 1).

In channel flow, where velocity gradient $\partial U_2/\partial x_2$ is dominant, production of normal Reynolds stresses in direction of flow prevail ($\partial U_2/\partial x_2 \rightarrow \mathcal{P}^{U}_{\tau,22} \rightarrow \tau_{22}$, Tab. 2). Terms for redistribution of energy (11, 12), that describe processes of redistribution of turbulent energy to other two directions, that is, terms $\mathcal{R}^{I}_{\tau,ij}$ and $\mathcal{R}^{II}_{\tau,ij}$ are modeled to diminish the effective generation of normal stress (τ_{22}) by redistributing it equally to the other two directions ($\tau_{22} \rightarrow \tau_{11}$ and $\tau_{22} \rightarrow \tau_{33}$, Tab. 2). Near the wall, where the process of redistribution of turbulent velocity fluctuations normal to the wall to other directions goes on, both wall-corrections term $\mathcal{R}^{I,\mathrm{w}}_{\tau,ij}$, $\mathcal{R}^{II,\mathrm{w}}_{\tau,ij}$ (9, 10), become "active", and in accordance to real physical situation describe redistribution of turbulent energy normal to the wall (τ_{33}) to other two directions ($\tau_{33} \rightarrow \tau_{11}$ and $\tau_{33} \rightarrow \tau_{22}$).

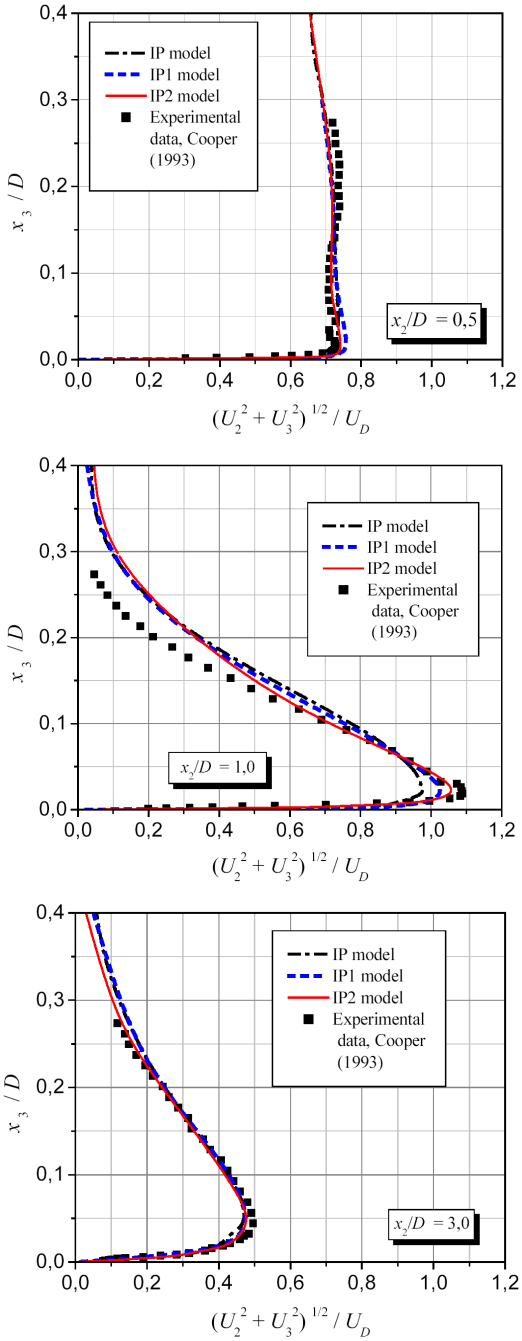

Figure 5. Mean velocity profiles in radial wall jet $Z/D = 2$, $\overline{\mathrm{Re}}_D = 23000$

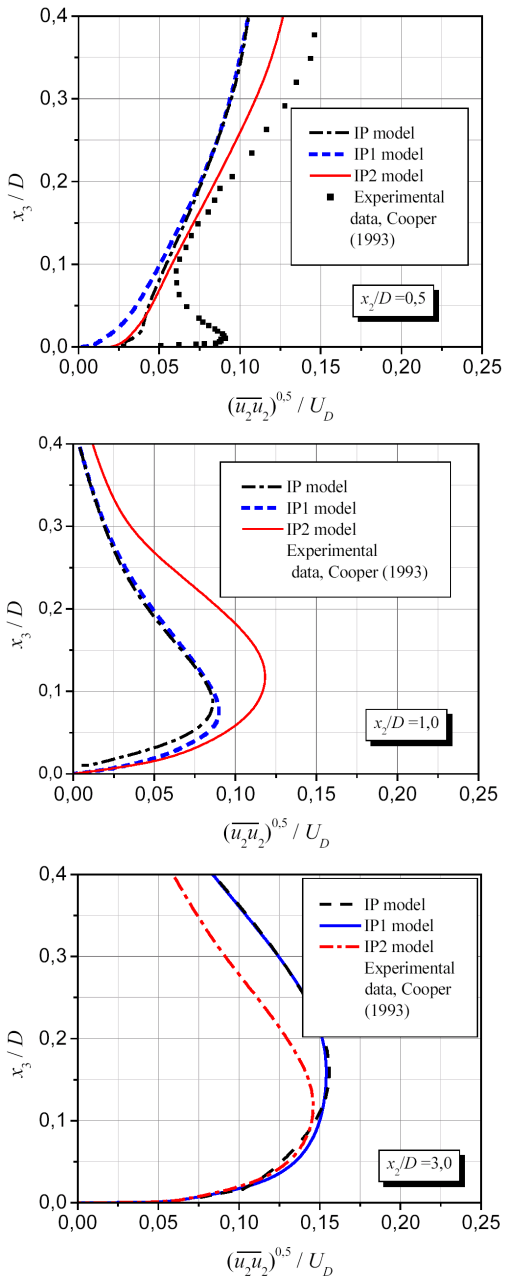

Figure 6. Profiles of r.m.s. turbulent velocity in radial wall jet – component parallel to wall, $Z/D=2$, $\overline{\mathrm{Re}}_D = 23000$

In this case of impinging flow (Fig. 1) turbulent kinetic energy generation arises mainly from velocity gradient $\partial U_3/\partial x_3$ ($\partial U_3/\partial x_3 \rightarrow \mathcal{P}^U_{\tau,33} \rightarrow \tau_{33}$, Tab. 3). Hence term $\mathcal{R}^{II}_{\tau,22}$, in redistributing this production, "acts" to decrease the stress normal to the wall ($\tau_{33} \rightarrow \tau_{22}, \tau_{33} \rightarrow \tau_{11}$, Tab. 3). It therefore follows that the form of $\mathcal{R}^{II,\mathrm{w}}_{\tau,ij}$ in equations (10) acts to reverse this $\mathcal{R}^{II}_{\tau,ij}$ effect and hence increase the production of the stress normal to the wall τ_{33}. These physically non-existing increasing components of Reynolds stress normal to the wall in the vicinity of the stagnation point leads to wrong, too excessive predictions of local Nusselt number (Fig. 8).

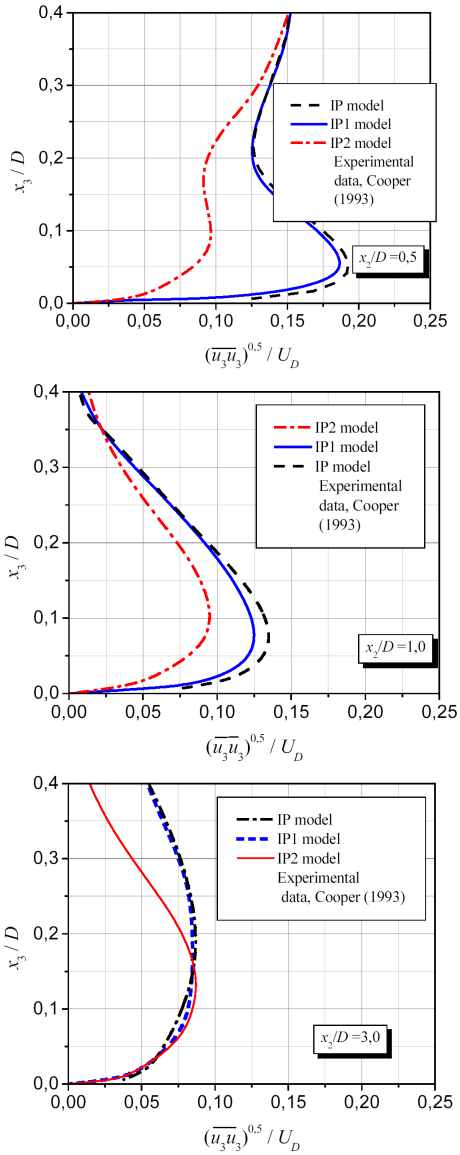

Figure 7. Profiles of r.m.s. turbulent velocity in radial wall jet – component normal to wall, $Z/D=2$, $\overline{\mathrm{Re}}_D = 23000$

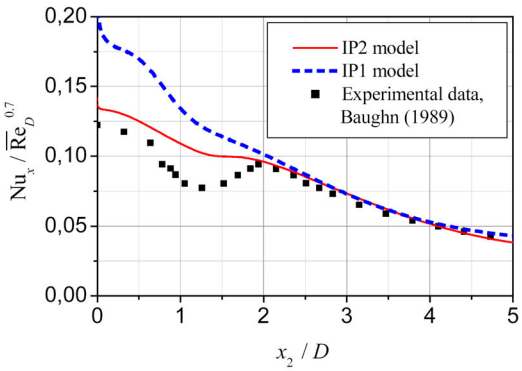

Figure 8. Variation of scaled Nusselt number with radius, $Z/D=2$, $\overline{\mathrm{Re}}_D = 23000$

The adverse effect that standard form of $\mathcal{R}^{II,\mathrm{w}}_{\tau,ij}$ exerts to predictions of the velocity and temperature characteristics of the impinging jet is thus seen to be intrinsic. That indicates necessity for different formulation of the wall-reflection model which should be sought that will damp the stress normal to the

wall irrespective of the main strain field.

Before attempting to formulate a wall-reflection term that gives the correct behaviour in an impinging flow, it was considered what constraints and guiding principles can be applied.

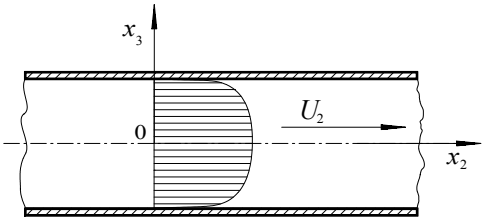

Figure 9. Flow field of channel flow (schematic)

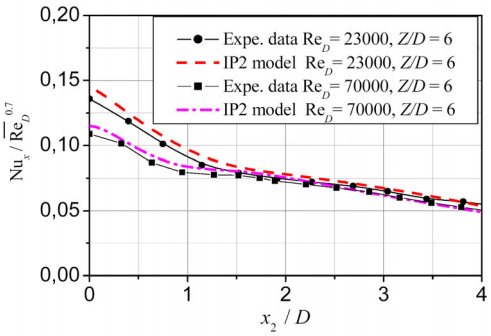

Figure 10. Variation of scaled Nusselt number with radius, $Z/D = 6$, $\overline{\mathrm{Re}}_D = 23000$ **and** $\overline{\mathrm{Re}}_D = 70000$

Obviously, the model for that new term $\mathcal{R}_{\tau,ij}^{II,\mathrm{w}}$ must be redistributed amongst the normal stresses, so ${}^{*}\mathcal{R}_{\tau,kk}^{\mathrm{w},II} = 0$, and it should be such that the stress normal to the wall is always damped. Also, as the wall-reflection process is mainly due to mean-strain influences, and it thus makes sence to require that the new terms would be products of mean velocity gradients and Reynolds stresses. In attempting to find the appropriate term, and as some of the previously cited characteristics possess mainly wall-reflection terms, the solution was carried out analyzing the known "nonstandard" rapid wall-reflection terms.

As only the term proposed by Craft (1991) was possessed desired characteristic, this term was accepted as the new wall-reflection term. In that way, the new model for pressure-strain correlation has form:

$$\mathcal{R}_{\tau,ij} = \mathcal{R}_{\tau,ij}^{I} + \mathcal{R}_{\tau,ij}^{II} + \mathcal{R}_{\tau,ij}^{\mathrm{w},I} + \mathcal{R}_{\tau,ij}^{\mathrm{w},II} + {}^{*}\mathcal{R}_{\tau,ij}^{\mathrm{w},II} \quad (29)$$

where ${}^{*}\mathcal{R}_{\tau,ij}^{II,\mathrm{w}}$ is modeled as:

$${}^{*}\mathcal{R}_{\tau,ij}^{\mathrm{w},II} = \rho\, C_{\mathrm{w}2}^{*} f_{\mathrm{w}} \frac{\partial U_l}{\partial x_m} n_l n_m \left(n_i n_j - \frac{1}{3} n_q n_q \delta_{ij}\right) \quad (30)$$

and where empirical constant $C_{\mathrm{w}2}^{*}$ has value $C_{\mathrm{w}2}^{*} = 0{,}3$. This new model was marked as IP2 model.

Subsequent numerical simulation derived by using that new IP2 model showed significant improvements in predicting normal Reynolds stresses field as well as local Nusselt number (Fig. 5, 6, 7 and 8). Similar numerical results were obtained by calculation with this IP2 model in cases of all other different regimes of flow (Fig 10).

9. CONCLUSION

The impinging jet calculations have highlighted a serious failure of standard wall-reflection model which can actually lead to "increase" of the stress normal to the wall in an impinging flow. This deficiency has been overcome by using a new, additional wall-reflection term ${}^{*}\mathcal{R}_{\tau,ij}^{\mathrm{w},II}$, that gives the required behavior in an impinging flow and does not violate the more conventional situation where the mean flow is parallel to the wall. With the addition of this term, the new model shows significant improvements in velocity, stress and heat-transfer predictions.

REFERENCES:

1. Banjac, M.: *Heat transfer in an Axisymetric Turbulent Impingig Jet*, Ph. D. Thesis, Faculty of Mechanical Engineering, University of Belgrade, Serbia, 2004.
2. Baughn, J.W.B. and Shimizu, S.: Heat Transfer Measurments From a Surface With Uniform Heat Flux and an Impinging Jet, Transactions of the ASME, Journal of Heat Transfer, Vol. 111, pp. 1096-1998, 1989.
3. Baughn, J.W.B., Yan, X. and Masbah, M.: *The effect of Reynolds number on the heat transfer distribution from a flat plate to an impinging jet*, ASME winter annual meeting, 1992.
4. Craft, T.I.: *Second-moment modeling of turbulent scalar transport*, Ph. D. Thesis, Faculty of Technology, University of Manchester, UK, 1991.
5. Daly, B.J. and Harlow, F.H.: Transport equations in turbulence, Physics of Fluids, Vol. 13, pp. 2634-2649, 1970.
6. Hanjalić, K. and Launder, B.E.: Contribution towards a Reynolds-stress closure for low-Reynolds-number turbulence, Journal of Fluid Mechanics, Vol. 74, Part. 4, pp. 593-610, 1976.
7. Holger, M.: Heat and Mass Transfer between Impinging Gas Jet and Solid Surfaces, Advances in Heat Transfer, Vol.13, pp. 1-60, 1977.
8. Launder, B.E., Reece, G.J. and Rodi, W.: Progress in the development of a Reynolds stress turbulence closure, Journal of Fluid Mechanics, Vol. 68, pp. 537- 566, 1975.
9. Rotta, J.C.: "Statistiche Theorie Nicht-homogener Turbulenz", Zeitschrift für Physik, Vol. 131, pp. 51-77, 1951.
10. Shir, C.C.: A Preliminary Numerical Study of Atmosferic Turbulent Flows in the Idealized Planetary Layer, Journal of Atmospheric Sciences, Vol. 30, pp. 1327-1339, 1973.
11. Spalding, B.: *PHOENICS Encyclopedia*, CHAM, London, UK, 1999.
12. Viskanta, R.: Heat transfer to Impinging Isothermal Gas and Flame Jets, Experimental Thermal and Fluid Science, Vol. 6, pp. 111-134, 1993.
13. Younis, B.A.: *On modeling the effects of streamline curvature on turbulent shear flows*, Ph. D. Thesis, University of London, UK, 1984.

NOMENCLATURE

a_{f}	thermal diffusivity for fluid, $a_{\mathrm{f}} = \lambda_{\mathrm{f}}/(\rho c_p)$
c_p	specific heat capacity at constant volume
D	jet pipe diameter
h_x	local heat transfer coefficient
H	mean specific enthalpy
k	turbulent kinetic energy
n_i	component of unit vector normal to wall

Nu_x local Nusselt number, $\mathrm{Nu}_x = \varphi D/[\lambda_\mathrm{f}(T_\mathrm{s} - T_\mathrm{amb})] = h_x D/\lambda_\mathrm{f}$

Pr_f Prandtl number

$\overline{\mathrm{Re}}_D$ Reynolds number based on bulk velocity and pipe diameter, $\overline{\mathrm{Re}}_D = DU_D/\nu_\mathrm{f}$

T_amb ambiance-jet air temperature

T_s wall surface temperature

U_i mean velocity components

u_i fluctuating velocity components

U_τ friction velocity $U_\tau = \sqrt{\tau_w/\rho}$

U_D jet bulk velocity

Z jet-to-plate distance

x_2 radial distance or coordinate parallel to impingement plate

x_2 axial distance or coordinate normal to impingement plate

y^+ non-dimensional distance, $y^+ = U_\tau y_\mathrm{n}/\nu_\mathrm{f}$

Greek symbols

δ_{ij} Kronecker delta

ε dissipation rate of turbulent kinetic energy

$\hat{\varepsilon}$ isotropic dissipation rate of turbulent kinetic energy

λ_f thermal conductivity for fluid

ν_f kinematic viscosity for fluid

ρ fluid density

τ_{ij} Reynolds or turbulent stress $\tau_{ij} = -\rho\overline{u_i u_j}$

τ_w wall shear stress $\tau_\mathrm{w} = \mu_\mathrm{f}(\partial U/\partial y)_{y=0}$

РАЗВОЈ НОВОГ НАПОНСКОГ МОДЕЛА ТУРБУЛЕНТНИХ НАПОНА ЗА ПРЕДВИЂАЊЕ ПРОЦЕСА ПРЕЛАЖЕЊА ТОПЛОТЕ ПРИ УДАРУ МЛАЗА У РАВНУ ЗАГРЕЈАНУ ПЛОЧУ

Милош Бањац, Богосав Васиљевић

У овом раду је представљен нов напонски модел (модел другог реда) турбулентних напона. Овај нови напонски модел настао је претварањем "стандардног" ИП (high-Reynolds) напонског модела у одговарајући напонски модел којим је могуће вршити прорачуне и у областима струјања са малим вредностима Рејнолдсовог турбулентног броја (low-Reynolds model), као и са поправком тог модела у виду допунског члана нагле прерасподеле турбулентних напона услед присуства зида ${}^*\mathcal{R}_{\tau,ij}^{II,\mathrm{w}}$. Претварање ИП модела из његове high-Reynolds у његову low-Reynolds верзију, извршено је укључивањем претходно занемарног утицаја молекуларне дифузије на процесе преношења, тј. са увођењем одговарајућих чланова и функција у једначину "преношења" Рејнолсових напона и једначину "преношења" дисипације турбулнтне кинетичке енергије. Нови, допунски члан нагле прерасподеле турбулентних напона услед присуства зида ${}^*\mathcal{R}_{\tau,ij}^{II,\mathrm{w}}$, који је моделиран у складу са реалном физичком ситуацијом, обухватио је нетипичан, такозвани ефекат еха притиска, тј. нетипичан процес прерасподеле турбулентних напона који се јавља у струјном пољу при удару млаза о плочу у близини зауставне тачке. Насупрот "стандардним" линеарним двоједначинским моделима турбулентних напона, предложени напонски модел даје квалитативно боља предвиђања поља кинетичке енергије турбуленције и значајно боља предвиђања локалних вредности Нуселовог броја. У поређењу са "стандардним" high-Reynolds напонским моделима, предложени модел показује значајно боља предвиђања турбулентних напона у зауставној зони удара млаза, нешто боља предвиђања поља осредњених брзина, а и омогућава предвиђање локаних вредности Нуселтовог броја.

Table 2. "Contribution" of corresponding terms to intensity of velocity fluctuations in channel flow

Term	Normal components of Reynolds stress		
	$\overline{u_1u_1}$	$\overline{u_2u_2}$	$\overline{u_3u_3}$
$-\mathcal{P}_{\tau,ij}^{U}/\rho$	0	$-2\overline{u_2u_3}\cdot\partial U_2/\partial x_3$	0
$-\mathcal{R}_{\tau,ij}^{II}/\rho$	$-0,4\overline{u_2u_3}\dfrac{\partial U_2}{\partial x_3}$	$0,8\overline{u_2u_3}\dfrac{\partial U_2}{\partial x_3}$	$-0,4\overline{u_2u_3}\dfrac{\partial U_2}{\partial x_3}$
$-\mathcal{R}_{\tau,ij}^{\mathrm{w},II}/\rho$	$-0,12f_\mathrm{w}\overline{u_2u_3}\dfrac{\partial U_2}{\partial x_3}$	$-0,12f_\mathrm{w}\overline{u_2u_3}\dfrac{\partial U_2}{\partial x_3}$	$0,24f_\mathrm{w}\overline{u_2u_3}\dfrac{\partial U_2}{\partial x_3}$

Table 3. "Contribution" of corresponding terms to intensity of velocity fluctuations in impinging flow

Term	Normal components of Reynolds stress		
	$\overline{u_1u_1}$	$\overline{u_2u_2}$	$\overline{u_3u_3}$
$-\mathcal{P}_{\tau,ij}^{U}/\rho$	0	$-2\overline{u_2u_2}\dfrac{\partial U_2}{\partial x_2}$	$-2\overline{u_3u_3}\dfrac{\partial U_3}{\partial x_3}$
$-\mathcal{R}_{\tau,ij}^{II}/\rho$	$-0,4\overline{u_2u_2}\dfrac{\partial U_2}{\partial x_2}-0,4\overline{u_3u_3}\dfrac{\partial U_3}{\partial x_3}$	$0,8\overline{u_2u_2}\dfrac{\partial U_2}{\partial x_2}-0,4\overline{u_3u_3}\dfrac{\partial U_3}{\partial x_3}$	$-0,4\overline{u_2u_2}\dfrac{\partial U_2}{\partial x_2}+0,8\overline{u_3u_3}\dfrac{\partial U_3}{\partial x_3}$
$-\mathcal{R}_{\tau,ij}^{\mathrm{w},II}/\rho$	$-0,12f_\mathrm{w}\overline{u_2u_2}\dfrac{\partial U_2}{\partial x_2}+0,24f_\mathrm{w}\overline{u_3u_3}\dfrac{\partial U_3}{\partial x_3}$	$-0,12f_\mathrm{w}\overline{u_2u_2}\dfrac{\partial U_2}{\partial x_2}+0,24f_\mathrm{w}\overline{u_3u_3}\dfrac{\partial U_3}{\partial x_3}$	$0,24f_\mathrm{w}\overline{u_2u_2}\dfrac{\partial U_2}{\partial x_2}-0,48f_\mathrm{w}\overline{u_3u_3}\dfrac{\partial U_3}{\partial x_3}$